

THE $\sqrt{42}$ m ELECTRO-OPTIC MODULATOR AS A FREQUENCY TRANSMITTER AND AS A FREQUENCY DOUBLER*

V. MANEA¹, M. MOGÎLDEA²

Faculty of Physics, University of Bucharest, P.O. Box MG-11,
0771253 Bucharest – Măgurele, Romania
E-mail: ¹vladimir.manea@yahoo.com
²marian_mogildea@yahoo.com

(Received September 1, 2008)

Abstract. A theoretical and experimental analysis of two applications of the $\sqrt{42}$ m electro-optic modulator is performed in the time and in the frequency domains. The analysis refers to the case of a harmonic electric input signal. The two applications are that of frequency transmitter, when the modulation is linear and the output signal has the same frequency as the modulating voltage, and that of frequency doubler, when the modulation is not linear but the output is a clean harmonic signal with twice the modulating frequency. Experimental recordings of the output signal and of its frequency spectrum are given, as function of the amplitude of the modulating voltage. The recordings are presented in comparison to some graphical representations of the output, resulting from the theoretical considerations. By means of a Bessel analysis, conditions for achieving single-frequency outputs are obtained.

Key words: electro-optic modulation, light polarization, spectral analysis, polarization dynamics.

1. INTRODUCTION

The modulation of the state of optical polarization is widely encountered in fields like the optical transmission of information [1] and the dynamic ellipsometry [2]. The purpose of the modulation process, depending on the application for which it is performed, can be either to obtain an output signal which is undistorted with respect to the one applied at the input [3], as in the optical transmission of information, or to obtain certain information from the nonlinearities which occur in the process, as modifications of the spectral structure of the output signal with respect to the one performing the modulation [4]. This last situation is of interest in the dynamic ellipsometry.

* Paper presented at the Annual Scientific Conference, June 6, 2008, Faculty of Physics, Bucharest University, Romania.

The polarization state modulation can be performed in a variety of ways, some of them being presented in Refs. [5–7]. What we will theoretically and experimentally analyze is the longitudinal electro-optic effect in crystals of class $\bar{4}2m$. The modulation process is performed by applying on the crystal a harmonic time-varying voltage and is converted in intensity modulation by using at the output a detector which is a square-law converter. A continuous voltage is simultaneously applied in order to set the point on the transmission characteristic of the crystal in the vicinity of which the modulation process will take place.

Depending on this point, one can distinguish some particular cases, two of which will be analyzed: the case in which the modulation is performed at the middle of the linear portion of the transmission characteristic and the case in which the modulation is performed at the bottom of the transmission characteristic (with no continuous voltage on the crystal). A low-amplitude input signal leads to different outputs in the two above mentioned situations. In the first, the output is a clean harmonic signal having the same frequency as the modulating voltage, which makes the modulator function as a frequency transmitter (linear modulation). In the second, the output is a clean harmonic signal with twice the modulating frequency, which makes the modulator function as a frequency doubler.

In both situations, the increase of the amplitude of the modulating voltage can lead to a modification of the time-varying form and spectral structure of the output signal. This modification will also be an object of our theoretical and experimental analysis, because, in certain applications, as we have previously mentioned, the nonlinearities of the modulation process have a practical importance.

2. THE MODULATION ARRANGEMENT

The modulation arrangement is presented in Fig. 1, in which A is an ADP electro-optic crystal. The modulation is performed by applying a voltage between two semitransparent electrodes, placed on the anterior and posterior sides of the crystal (with respect to the OZ axis). By construction, the electrically induced axes of the crystal ($O'X'$, $O'Y'$) make a 45° angle with the major axis of the input polarizer IP . The output polarizer OP has the role of selecting the linear polarization component of the modulated light, to be detected by the photo-detector PD .

The applied voltage has a continuous and also a time-varying component,

$$U = U_0 + U_m \sin \Omega t, \quad (1)$$

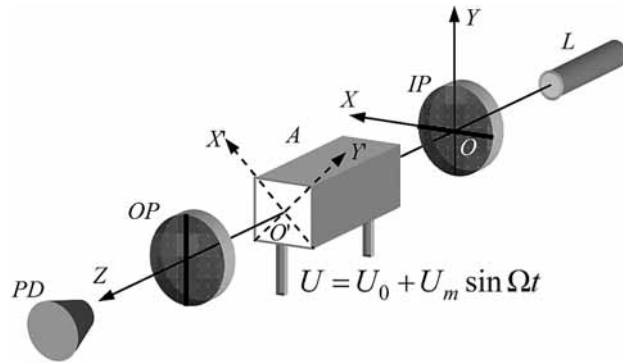
and by the electro-optic effect it determines the appearance of a retardance 2δ between the linear polarization components along the two electrically induced axes of the crystal. The retardance will also have a constant term, $2\delta_0$, and a harmonic one, of amplitude 2Γ , given by the formulae:

$$2\delta_0 = \frac{2\pi}{\lambda_0} n_0^3 r_{63} U_0 = \pi \frac{U_0}{U_{\lambda/2}} \quad \text{and} \quad 2\Gamma = \frac{2\pi}{\lambda_0} n_0^3 r_{63} U_m = \pi \frac{U_m}{U_{\lambda/2}}, \quad (2)$$

where n_0 is the refractive crystalline index in the absence of any voltage, r_{63} is one of the non-vanishing electro-optic coefficients for a crystal of class $\bar{4}2m$ and λ_0 is the vacuum wavelength of the incident light. $U_{\lambda/2}$ is the voltage for which the induced retardance is π , known as the half-wave voltage of the crystal. Thus, the expression of the phase difference is:

$$2\delta = 2\delta_0 + 2\Gamma \sin \Omega t = 2\delta_0 + \pi \frac{U_m}{U_{\lambda/2}} \sin \Omega t. \quad (3)$$

Fig. 1 – Modulation arrangement:
L – Laser light source; *IP* – input polarizer;
A – ADP modulator;
OP – output polarizer; *PD* – photo-detector.



3. THEORETICAL ANALYSIS

We consider the light beam monochromatic and totally polarized, making the Jones formalism well suited for its description. Because the major axis of the input polarizer is set horizontally, we will perform the calculi in the OXY coordinate system, which provides less complicated results.

The Jones matrix \mathbf{M} of the modulator is that of a linear retarder with 45° azimuth and variable retardance,

$$\mathbf{M} = \begin{bmatrix} \cos \delta & i \sin \delta \\ i \sin \delta & \cos \delta \end{bmatrix}, \quad (4)$$

which leads to the following reduced Jones vector of the modulated light:

$$\begin{bmatrix} E_{ox} \\ E_{oy} \end{bmatrix} = \mathbf{M} \begin{bmatrix} e^{i\omega_0 t} \\ 0 \end{bmatrix} = \begin{bmatrix} \cos(\delta_0 + \Gamma \sin \Omega t) \\ i \sin(\delta_0 + \Gamma \sin \Omega t) \end{bmatrix} =$$

$$= \left[\begin{array}{l} \cos \delta_0 \sum_{k=-\infty}^{\infty} J_{2k}(\Gamma) e^{i[\omega_0+2k\Omega]t} + e^{i\frac{\pi}{2}} \sin \delta_0 \sum_{k=-\infty}^{\infty} J_{2k-1}(\Gamma) e^{i[\omega_0+(2k-1)\Omega]t} \\ e^{i\frac{\pi}{2}} \sin \delta_0 \sum_{k=-\infty}^{\infty} J_{2k}(\Gamma) e^{i[\omega_0+2k\Omega]t} + \cos \delta_0 \sum_{k=-\infty}^{\infty} J_{2k-1}(\Gamma) e^{i[\omega_0+(2k-1)\Omega]t} \end{array} \right] \quad (5)$$

where $J(\Gamma)$ are the Bessel functions of the first kind.

The phase difference between the different harmonic components of the modulated light is not constant in time, because their angular frequencies are different. Nevertheless, after a period of $2\pi/\Omega$, any relative phase configuration is reproduced, so that the spectral components are coherent, in the sense of generalized coherence [9], which determines the beats at the intensity level and, more generally, in a spatio-temporal detection, of the intensity waves [10].

The electrical signal given by the photo-detector is directly proportional to the intensity of the light beam emerging from the output polarizer. The intensities of the polarization components E_{ox} and E_{oy} have the following expressions, which can also be considered, without changing the notation, as expressions of the output signal, obtained by a proper positioning of the output polarizer:

$$\begin{aligned} I_{ox} &= \frac{1}{2} |E_{ox}|^2 = \frac{1}{2} \cos^2(\delta_0 + \Gamma \sin \Omega t) \\ I_{oy} &= \frac{1}{2} |E_{oy}|^2 = \frac{1}{2} \sin^2(\delta_0 + \Gamma \sin \Omega t). \end{aligned} \quad (6)$$

The harmonic structure of the two time-varying forms is the following:

$$\begin{aligned} I_{ox,oy} &= \frac{1}{4} \left\{ 1 \pm \cos 2\delta_0 \left[J_0(2\Gamma) + 2 \sum_{n=1}^{\infty} J_{2n}(2\Gamma) \cos 2n\Omega t \right] \mp \right. \\ &\quad \left. \mp \sin 2\delta_0 \left[2 \sum_{n=1}^{\infty} J_{2n-1}(2\Gamma) \sin(2n-1)\Omega t \right] \right\}. \end{aligned} \quad (7)$$

As one can see in the above expression, the output signal generally has a complex form, containing, apart from the fundamental modulation frequency, all its odd and even harmonics. Their amplitudes depend on the values of the Bessel function in $2\Gamma = \pi U_m / U_{\lambda/2}$, so that the higher order harmonics appear by increasing the amplitude of the modulating voltage. The signals corresponding to the two orthogonal polarization components only differ by a 180° relative phase shift.

Thus, the analysis of the nonlinearities which occur in the modulation process, or of the conditions for achieving a clean harmonic output, imposes the substitution of 2Γ in Eq. (7) by $\pi U_m / U_{\lambda/2}$ which introduces the relevant parameter for the analysis (not U_m , but the fraction it represents with respect to the half-wave voltage of the crystal).

As we have mentioned in the *Introduction*, we will focus on two particular cases, with respect to the value of the continuous component of the input signal. In the first case, there is no continuous voltage on the crystal ($U_0 = 0$), while in the second case, the value of the continuous voltage is equal to the quarter-wave voltage of the crystal ($U_0 = U_{\lambda/4} = U_{\lambda/2}/2$).

a) $U_0 = 0$. In this case, only the even order harmonics are present in the output signal:

$$I_{ox,oy} = \frac{1}{4} \left[1 \pm J_0 \left(\pi \frac{U_m}{U_{\lambda/2}} \right) \pm 2 \sum_{n=1}^{\infty} J_{2n} \left(\pi \frac{U_m}{U_{\lambda/2}} \right) \cos 2n\Omega t \right]. \quad (8)$$

For a low-amplitude modulation, the output is a clean harmonic signal with twice the modulating frequency. As the experimental recordings will confirm, in order to discuss the conditions for the output to be undistorted with respect to the harmonic form, one must only refer to the first two Bessel amplitudes of the different harmonics. For example, in Eq. (8), the fourth harmonic J_4 takes important values, distorting the signal, before the sixth begins to increase.

As a general condition for obtaining an undistorted output signal, we consider sufficient to have an amplitude of the modulating voltage for which the distorting Bessel amplitude is with at least two orders of value under the one of the main frequency. In the case of no continuous voltage, the main frequency is twice that of the modulating signal, while in the case in which U_0 is equal to the quarter-wave voltage, the main frequency is the modulation frequency itself. For making some quantitative evaluations, we will use the following approximation for the Bessel functions of small argument (which is the case in our discussion) [11]:

$$J_n(x) = \frac{1}{2^n n!} x^n. \quad (9)$$

As we have previously mentioned, the two relevant Bessel functions for the case of no continuous voltage are J_2 and J_4 , leading to the following condition for obtaining a clean double-frequency output signal:

$$J_4 / J_2 \leq 0.01 \Leftrightarrow \frac{\pi^2}{48} \left(\frac{U_m}{U_{\lambda/2}} \right)^2 \leq 0.01 \Rightarrow U_m \leq 0.22 U_{\lambda/2}. \quad (10)$$

This means that the amplitude of the modulating voltage must be less than 22% of the half-wave voltage of the crystal.

If the amplitude of the input signal is increased sufficiently, a “hump” is produced on the upper side of the output signal (Fig. 2). The condition for the occurrence of this situation can be obtained by performing the temporal derivative of the output signal and by imposing on it to have a point of annulment on the interval $(0, T/4)$, where T is the period of the modulating voltage:

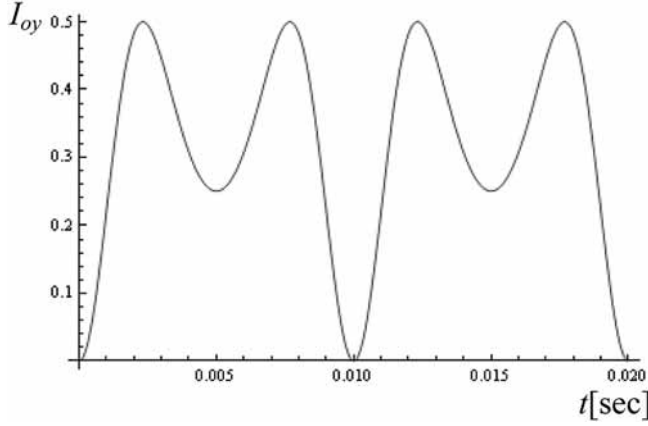


Fig. 2 – Theoretical representation of the asymmetric “humps”.

$$\frac{dI_{oy}}{dt} = 0 \Leftrightarrow \sin \left[\pi \frac{U_m}{U_{\lambda/2}} \sin(\Omega t) \right] \cos(\Omega t) = 0, \quad t \in \left(0, \frac{\pi}{2\Omega} \right). \quad (11)$$

This condition arises from the fact that the number of points of local extremum for the first quarter-period (open interval) is equal to the number of “humps”. The local extremum corresponding to the left “peak” (the one of interest) is determined by the annullment of the sine factor. This is possible for the first quarter-period only if $U_m > U_{\lambda/2}$. Thus, the first “hump” appears when the amplitude of the modulating voltage exceeds the half-wave voltage of the crystal.

If the amplitude of the input signal is increased even more, the “hump” becomes deeper, until it reaches the lower side of the output signal and a second “hump” begins to arise from it (Fig. 3). The general condition for the appearance of the n -th “hump” derives from considerations similar to the previous and requires for the amplitude of the modulating voltage to become n times greater than the half-wave voltage of the crystal.

b) $U_0 = U_{\lambda/4}$. The constant retardance $2\delta_0$ is $\pi/2$, so Eq. (7) becomes:

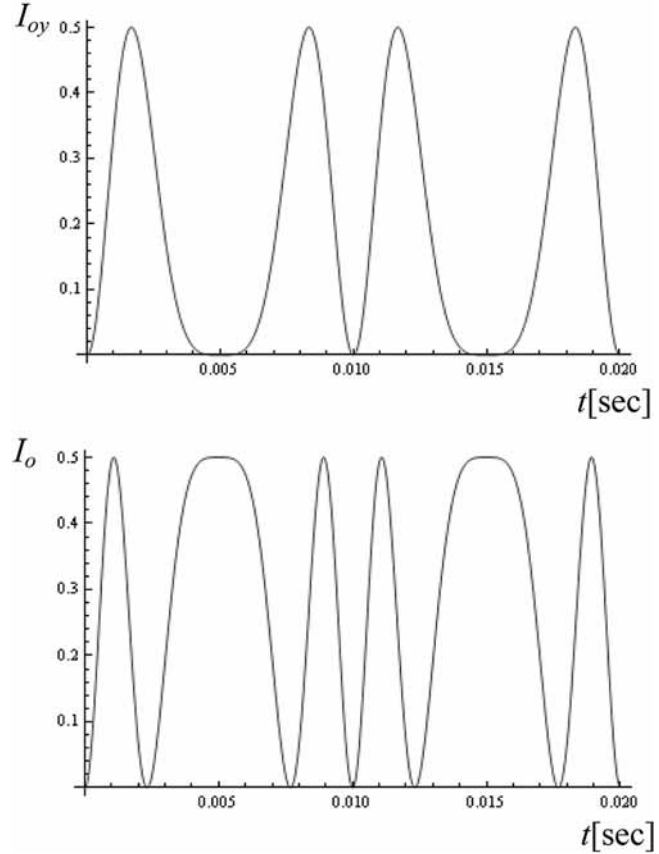
$$I_{ox,oy} = \frac{1}{4} \left[1 \mp 2 \sum_{n=1}^{\infty} J_{2n-1} \left(\pi \frac{U_m}{U_{\lambda/2}} \right) \sin(2n-1)\Omega t \right]. \quad (12)$$

In this case, only the odd harmonics are present in the spectrum of the output signal, so a linear modulation is possible. In this sense, the relevant Bessel functions are J_3 and J_1 , so, according to the general condition enounced at point a), in order to have a reasonably linear transmission of the signal, its amplitude must have a value that satisfies the following relation:

$$J_3 / J_1 \leq 0.01 \Rightarrow \frac{\pi^2}{24} \left(\frac{U_m}{U_{\lambda/2}} \right)^2 \leq 0.01 \Rightarrow U_m \leq 0.15 U_{\lambda/2}, \quad (13)$$

so it must be less than 15% of the half-wave voltage.

Fig. 3 – Theoretical representation of the output signal for $U_m = 2U_{\lambda/2}$ (upper) and $U_m = 3U_{\lambda/2}$ (lower).



By increasing the amplitude of the input signal beyond a certain limit, a pair of symmetric “humps” appears in the time-varying form of the output (Fig. 4). Again, the exact value of this limit can be obtained by performing the temporal derivative of the output signal and by imposing on it to have a point of annullment on the first quarter-period (open interval):

$$\frac{dI_{oy}}{dt} = 0 \Leftrightarrow \sin\left[\frac{\pi}{2} + \pi \frac{U_m}{U_{\lambda/2}} \sin(\Omega t)\right] \cos(\Omega t) = 0, \quad t \in \left(0, \frac{\pi}{2\Omega}\right). \quad (14)$$

This time, by analyzing the above condition, it results that the first pair of “humps” appears when the amplitude of the modulating voltage exceeds the quarter-wave voltage of the crystal ($U_m > U_{\lambda/2}/2$). The evolution of the humps with the increase of the amplitude of the input signal resembles that of the previous case, the difference being that this time the “humps” appear always in pairs. For the appearance of the n -th pair of “humps” the amplitude of the input signal must become $n-1/2$ times greater than the half-wave voltage of the crystal.

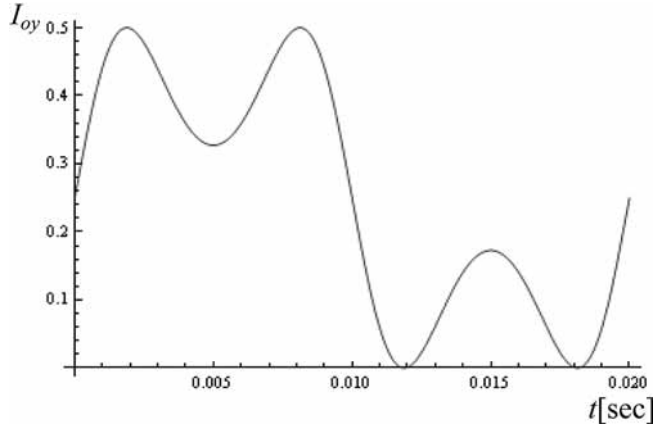


Fig. 4 – Theoretical representation of the symmetric “humps”.

4. EXPERIMENTAL RECORDINGS

For performing the experimental recordings, the employed photo-detector was connected to a computer, which was responsible for the acquisition and digital processing of the output signal. With the aid of a virtual oscilloscope program, the time-varying form of the output signal could be displayed on the monitor of the computer, together with its frequency spectrum. The images that we recorded are presented in this section.

Again, we refer to the particular cases in discussion ($U_0 = 0$ and $U_0 = U_{\lambda/4}$). As a general observation, the presented figures confirm the theoretical expectations, more specifically, in the first case only the even order harmonics appear in the frequency spectrum, while in the second, only the odd order ones.

a) $U_0 = 0$ – in Fig. 5 (upper) one can see the clean double-frequency output for low-amplitude modulation. The asymmetric “humps” are presented in Fig. 5 (lower), for an amplitude of the modulating voltage which exceeds the half-wave voltage of the crystal.

In Fig. 6, one can see the output signal for higher amplitudes of the modulating voltage, leading to the appearance of the higher order “humps”. The recordings correspond to one of the cases theoretically represented in Fig. 3, and one can see that they confirm the expectations.

b) $U_0 = U_{\lambda/4}$ – This is the case in which a linear process of modulation can be achieved for low amplitude modulating voltages (Fig. 7).

The distortions produced by increasing the amplitude of the input signal are presented in Fig. 8, more specifically the first pair of symmetric “humps” (upper), for an amplitude which exceeds the quarter-wave voltage of the crystal, and the second order pair of symmetric “humps” (lower), for an amplitude which exceeds by more than one and a half times the half-wave voltage. By analyzing Fig. 8 (upper),

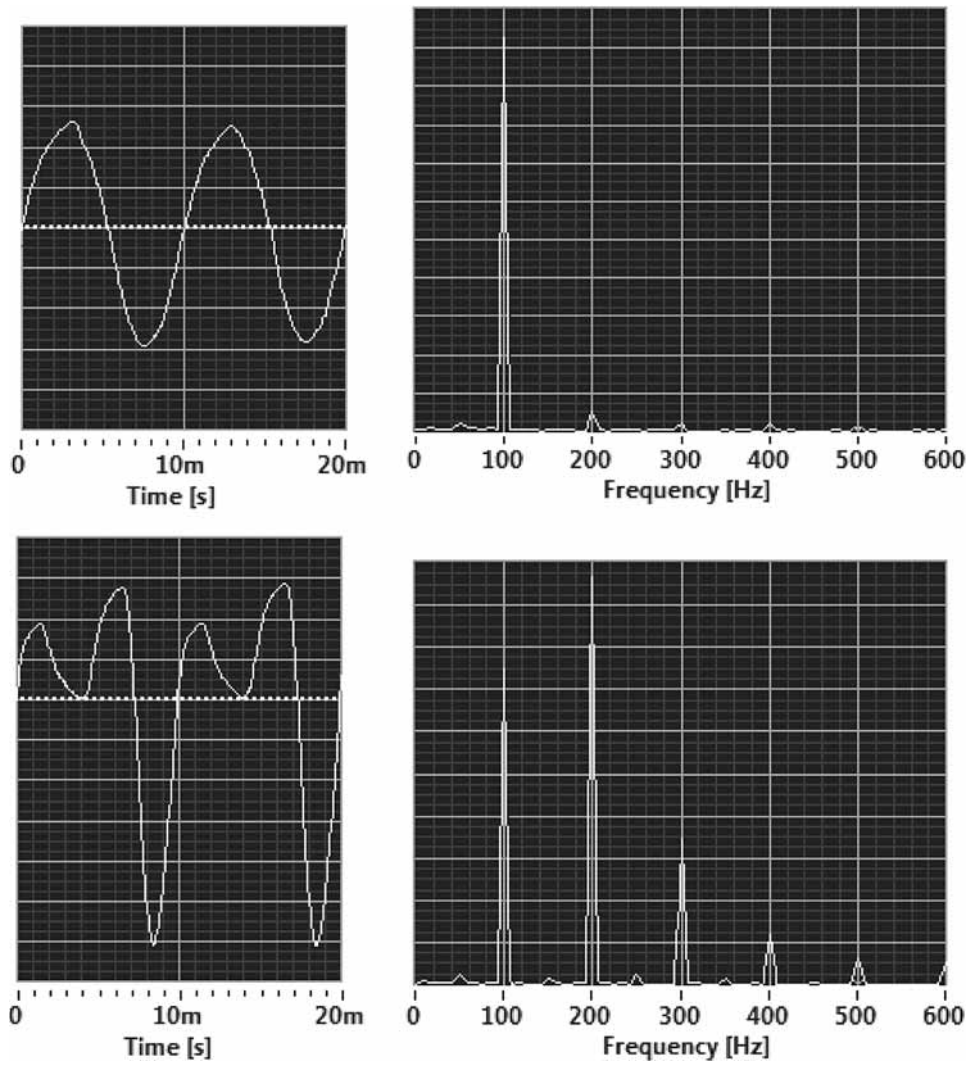


Fig. 5 – Double frequency output (upper) and asymmetric “humps” (lower) – $U_0 = 0$.

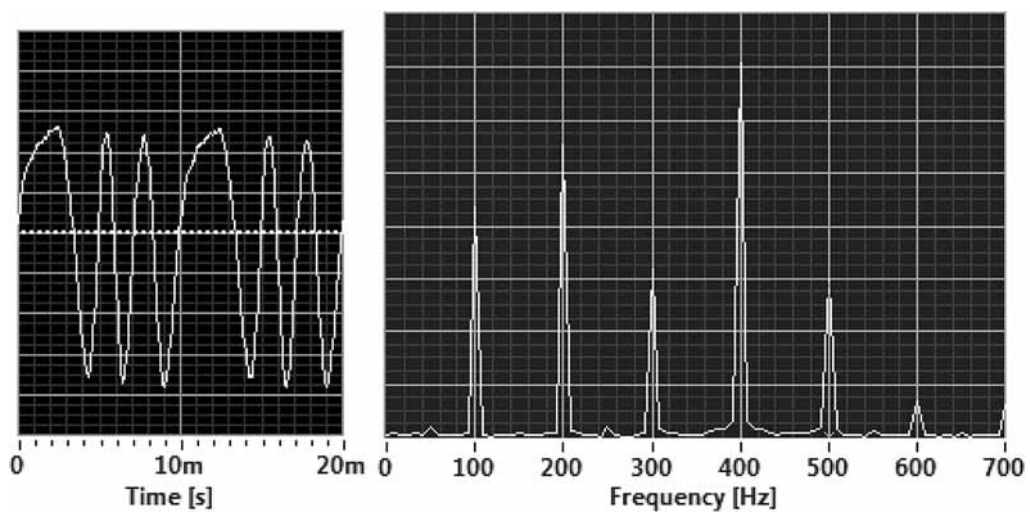


Fig. 6 – Output for $U_m = 3U_{\lambda/2}$ ($U_0 = 0$).

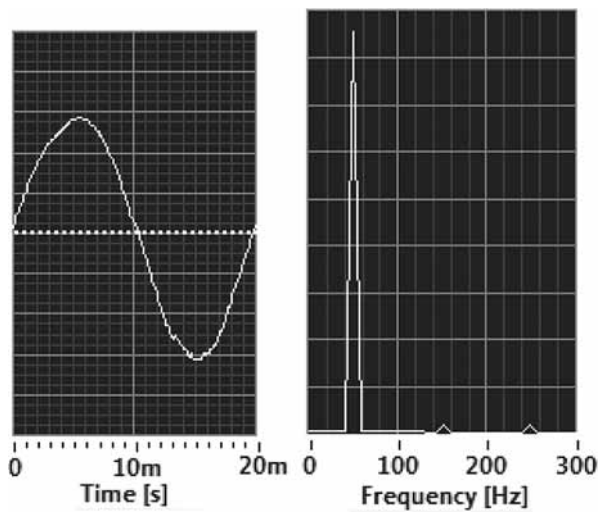


Fig. 7 – Output in the case of linear modulation ($U_0 = U_{\lambda/4}$).

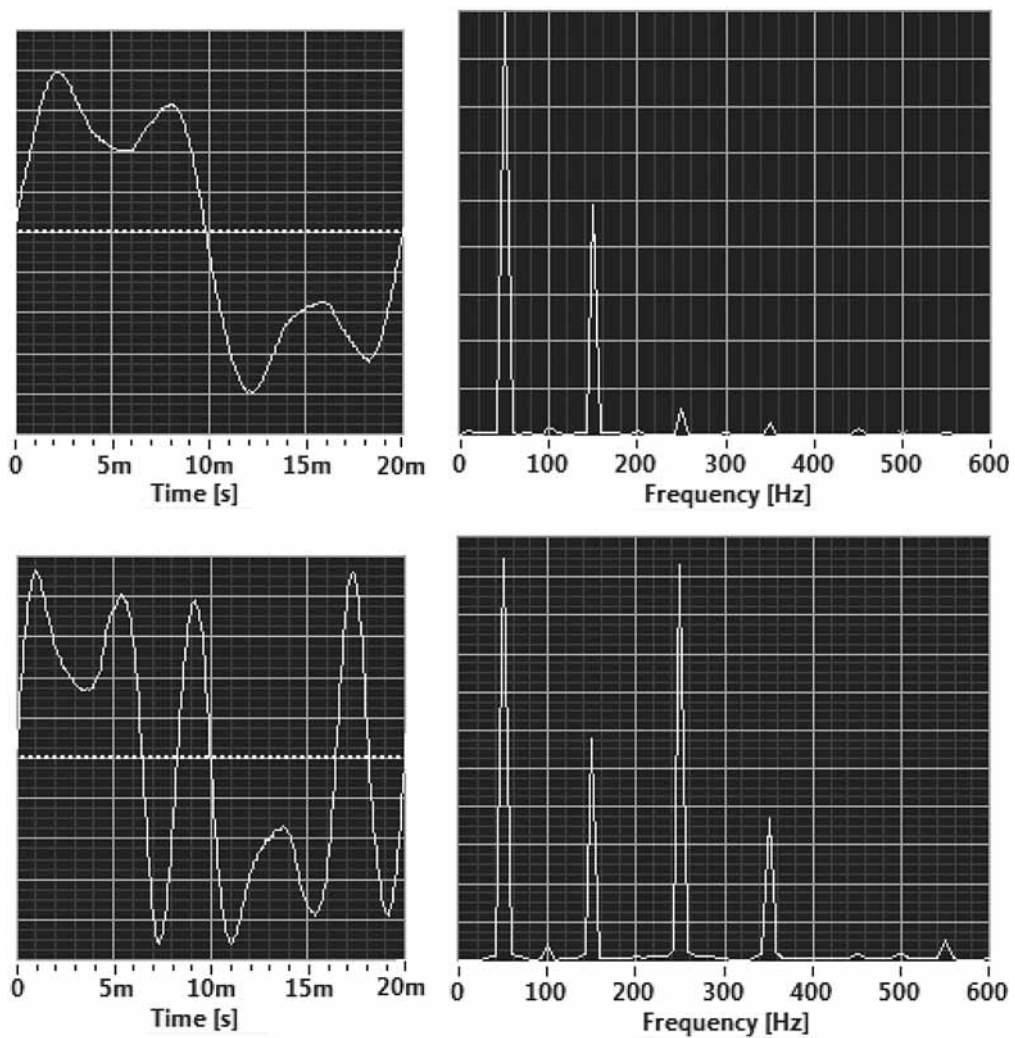


Fig. 8 – Symmetric “humps” (upper) and double “humps” (lower) output ($U_0 = U_{\lambda/4}$).

it becomes evident that the third harmonic is responsible for the distortion of the clean output signal in Fig. 7, before the amplitude of the fifth harmonic takes significant values.

5. CONCLUSIONS

The electro-optic modulator of type $\overline{42m}$ was theoretically and experimentally analyzed, as function of the two main controllable parameters: the continuous and the alternative voltage applied on the crystal. The output signal was directly proportional to the intensity of the beam emerging from the output polarizer, leading to the time-varying forms expressed in Eqs. (6).

The theoretical and experimental analysis was concentrated on two cases of modulation, corresponding to the most common values of the continuous voltage, $U_0 = 0$ and $U_0 = U_{\lambda/4}$. One could see that, in the two analyzed cases, the output signal contains either the even, or the odd harmonics, respectively.

By performing a Bessel analysis of Eqs. (8) and (12), conditions were achieved for obtaining a clean double frequency signal, when $U_0 = 0$, and for having a linear process of modulation, when $U_0 = U_{\lambda/4}$, in other words, for the modulator to function as a frequency doubler or as a frequency transmitter, respectively. Furthermore, the specific forms of the nonlinearities which occur in the modulation process were theoretically described (making also use of some graphical representations) and rigorous conditions were given for the obtainment of each specific form. The evolution of the modulation distortions was experimentally illustrated in the two mentioned cases, and the theoretical expectations were confirmed by the experimental recordings.

We equally emphasized in our analysis the linearity and the nonlinearities of the modulation process because of their practical importance. In the optical transmission of information, the interest is to obtain a high linearity of the modulation, with a greater tolerance for the amplitude of the input signal than the one offered by Eq. (13). This can be obtained, for example, by means of a multi-stage modulator, as is described in Ref. [3]. On the other hand, the modifications of the spectral structure of the output signal are important in the dynamic ellipsometry, where such modifications hold the relevant information concerning the analyzed system [12, 13].

REFERENCES

1. K.-P. Ho, *Phase-Modulated Optical Communication Systems*, Springer, New York, 2005.
2. G. E. Jellison, Jr., F. A. Modine, *Polarization Modulation Ellipsometry*, in: H. Tompkins, E. A. Irene (Eds.), *Handbook of Ellipsometry*, William Andrew Publ. Comp., New Jersey, 2005.

3. A. Garcia-Weidner, *Design of an ultralinear Pockles effect modulator: a successive approximation method based on Poincaré sphere analysis*, Appl. Opt., **32**, 7313–7325 (1993).
4. B. Szafraniec, R. Mästle, D. Baney, *Polarization mode dispersion measurement based on continuous polarization modulation*, Appl. Opt., **47**, 1109–1116 (2008).
5. K. Postava, A. Maziewski, T. Yamaguchi, R. Ossikovski, S. Visnovsky, J. Pistora, *Null ellipsometer with phase modulation*, Opt. Express, **12**, 6040–6045 (2004).
6. R. Chitaree, K. Weir, A. W. Palmer and K. T. V. Grattan, *A highly birefringent fibre polarization modulation scheme for ellipsometry: system analysis and performance*, Meas. Sci. Technol., **5**, 1226–1232 (1994).
7. T. Tudor, *Spectral analysis of the device operators. The rotating birefringent plate*, J. Opt. Soc. Am. A, **18**, 926–931 (2001).
8. T. Tudor, *Spectral analysis of the device operators in polarization dynamics*, J. Modern Opt., **48**, 1669–1689 (2001).
9. T. Tudor, *The generalized coherence of multifrequency optical fields*, Journal of Optics-Paris (Nouv. Rev. Opt.), **25**, 121–127 (1994).
10. T. Tudor, *Intensity waves in multifrequency optical fields*, Optik, **100**, 15–20 (1995).
11. F. W. J. Olver, *Bessel Functions of Integer Order*, in: M. Abramowitz, I. A. Stegun (Eds.), *Handbook of Mathematical Functions with Formulas, Graphs, and Mathematical Tables*, Dover Publ., New York, 1964.
12. A. E. Naciri, L. Johann, R. Kleim, *Spectroscopic generalized ellipsometry based on Fourier analysis*, Appl. Opt., **38**, 4802–4811 (1999).
13. B.-E. Benkelfat, E.-H. Horache, Q. Zou, B. Vinouze, *An electro-optic modulation technique for direct and accurate measurement of birefringence*, Opt. Comm., **221**, 271–278 (2003).